Electrochemistry of Azapropazone at a Gold Electrode in a Britton-Robinson Buffer Solution of pH 4.0

I. S. El-Hallag[1*], A. A. Al-Owais[2], S. H. El-Mossalamy[3] and H. A. M. Hendawy[4]

[1]*Chemistry Department, Faculty of Science, Tanta University, Tanta, Egypt*
[2]*Chemistry Department, Colleague of Science, King Saud University, Riyadh, Saudi Arabia*
[3]*Chemistry Department, Faculty of Science, Benha University, Benha, Egypt*
[4]*National Organization for Drug Control and Research, (NODCAR), Cairo, Egypt*
*Corresponding author: i.elhallag@yahoo.com

Received 03/02/2024; accepted 18/07/2024
https://doi.org/10.4152/pea.2026440203

Abstract
Herein, accurate voltammetric techniques were used for investigating Aza compound at an Au electrode in an aqueous universal BRB solution with pH 4.0 and at room temperature. Employed voltammetric methods were CV, ConvV and DeconvV, at various SR in the range from 40 to 800 mV/s. DSM was used to confirm experimental electrochemical parameters, and to identify the nature of the electrode reaction mechanistic pathway. Recorded CV revealed an uni-directional irreversible sharp anodic peak (E_p = 0.541 mV) in a BRB with pH 4.0. It indicated that the oxidation process was moderately fast. Electrons consumed in the electrode reaction were two. ConvV and DeconvV supported the presence of a chemical step coupled with electron transfer, due to the absence of the cathodic peak coupled in the reverse scan. Oxidative peak sharpness indicated some Aza adsorption control at the Au electrode surface.

Keywords: Aza; DSM; electrochemical parameters; electrode reaction; voltammetric techniques.

Introduction•

Aza non-steroidal anti-inflammatory medications include benzotriazine-1,3-dione [1-4]. By inhibiting cyclooxygenase, which transforms arachidonic acid into cyclic endoperoxides, precursors of prostaglandins, they prevent prostaglandins production. These drugs also have analgesic, antipyretic, platelet-inhibitory and anti-inflammatory effects, which are explained by the inhibition of prostaglandin synthesis. However, additional mechanisms may also be involved in their anti-inflammatory properties, Gold Shield produces it under brand name Rheumox [1].
British National Formulary 60 no longer includes Aza. Scheme 1 provides its molecular structure. It has a powerful anti-inflammatory effect by inhibiting the production of oxygen radicals that damage tissue, interleukin-1 produced by synovial tissue, the accumulation and possibly degranulation of leukocytes, and the release of autolytic enzymes from lysosomal bodies [5].

• The abbreviations list is in page 116.

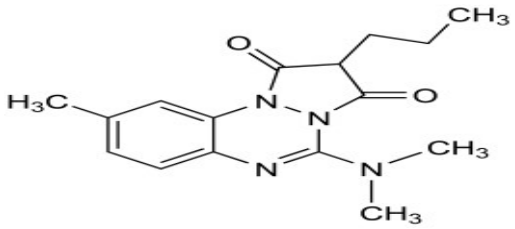

Scheme 1: Chemical structure of Aza.

Aza undergoes hepatic metabolism where it is transformed into its 8-hydroxy form (Mi307), in the same reactivity sequence as the parent molecule. There is a growing interest in using pharmaceutical substances for treating diseases and improving body functions. Huge numbers of new drugs are annually introduced, and up to date, more than 100,000 dosage forms and 10,000 medicinal substances are registered worldwide [6-9]. Monitoring the drug residues in pharmaceutical formulations, and their metabolites in bodily fluids, is of utmost importance for many research studies [10]. Different methods have been reported for Aza determination, including TLC [3] and HPLC [11-16]. While electrochemical approaches have shown to be particularly sensitive for the detection of organic compounds, including medicines and related chemicals in pharmaceutical dosage forms, and their oxidizeable properties, the majority of these technologies are either difficult to use or unavailable. Carbon electrodes, particularly GCE, are frequently used in electrochemical experiments, due to their low background current, large potential windows, chemical inertness, low cost and suitability for the detection of numerous organic and biological chemicals. They have been widely used, because of their distinct qualities, including their adaptability to chemical manipulation. To the best of our knowledge, there are no electrochemistry experiments on Aza at the Au electrode in an aqueous BRB solution as an impartial electrolyte. Aza examination employing CV, ConvV and DSM is therefore herein described. Experimental work was done to determine chemical and electrochemical parameters, and DSM was used to verify them. Thus, this article presents an electrochemical study of Aza at an Au electrode in a mildly acidic medium of a universal BRB solution with pH 4.0, using CV, ConvV-DeconvV transforms and DSM at various SR values.

Experimental

Chemicals

Aza was purchased from Egypt-based Delta Pharma Pharmaceutical Co., as-dried. The sample's purity was 99.8%. Aza was dissolved in 10 mL methanol, and the mixture was then completed to 50 mL in a measuring flask with bidistilled water, to yield 5 x 10^{-4} M stock solutions. For a week, the solutions were kept in a fridge. A universal BRB solution with pH 4.0 [17] was employed as supporting electrolyte. Analytical-grade reagents were used to create the solutions in bidistilled water. Prior to each electrochemical measurement, Au electrode was manually polished with 0.5 μm alumina powder on a smooth polishing cloth. Then, it was cleaned with double-distilled water and methanol, before being dried with tissue paper.

Instrumentation

Micro-Autolab type III systems were used to conduct electrochemical tests in a conventional 3-electrode cell (Eco Chemie, NL). An Au electrode disc, Ag/AgCl and Pt wire were employed as working, reference and counter electrode, respectively, with 3 M KCl. BRB pH was measured using a glass combination electrode and a digital pH/mV meter (JEANWAY 3510). Through the use of finite difference techniques, EG and G condesim software, data were examined by DSM. DSM software's algorithms were coded and applied. All measurements were performed at ambient temperatures.

Results and discussion

CV behaviour

CV experiment was conducted to understand voltammetric behaviour of Aza redox reactions on Au disc electrode. CV images of 5.0 x 10^{-6} M Aza on Au electrode at SR of 360 mV/s in a BRB with pH 4 are shown in Fig. 1.

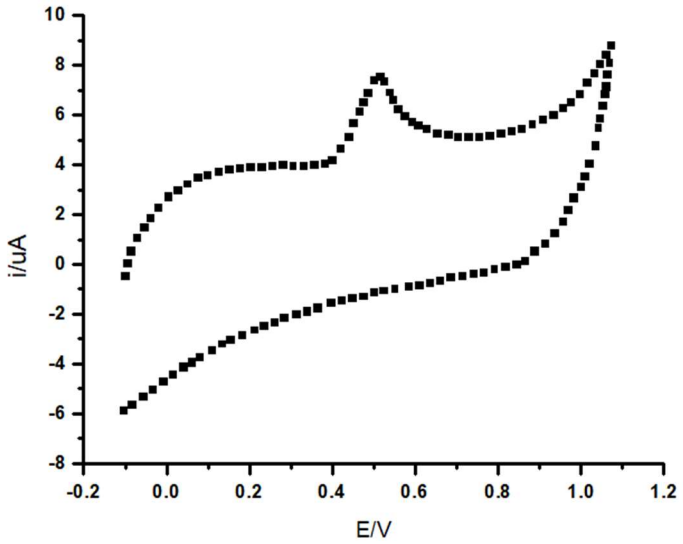

Figure 1: CV of 5.0 x 10^{-6} M Aza on Au electrode at a SR of 360 mV/s in a BRB with pH 4.

Aza revealed to be an electroactive drug during the initial scan. It was oxidised at Au electrode between 0.0 and 1.1 V, yielding one distinct, irreversible oxidation peak that could be seen at 0.544 V on the anodic scan. The absence of a reductive peak in the reverse scan established an irreversible electrochemical process paired with a quick chemical reaction immediately after electron transfer process.

Effect of SR

Fig. 2 shows that when SR rose, anodic i_p location shifted towards more positive potentials, and i_p height rose, which could be due to the somewhat quick electron transfer rate of the oxidative process at Au electrode. To understand the behaviour and reversibility of electrode reactions, the influence of SR potential on the electrochemical process was examined.

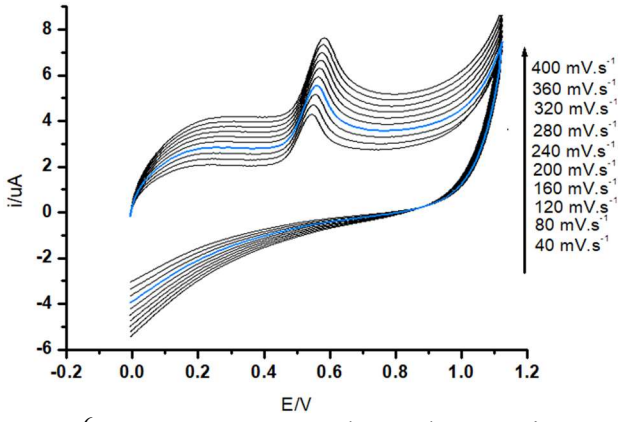

Figure 2: CV of 5.0 x 10^{-6} M Aza on an Au electrode at various SR in a BRB solution with pH 4.

A representation of anodic i_p obtained from a CV of 5 x 10^{-6} M Aza with pH 4.0, at the Au electrode, using SR square root "(*v*)1/2" and SR "(*v*)" is shown in Fig. 3.

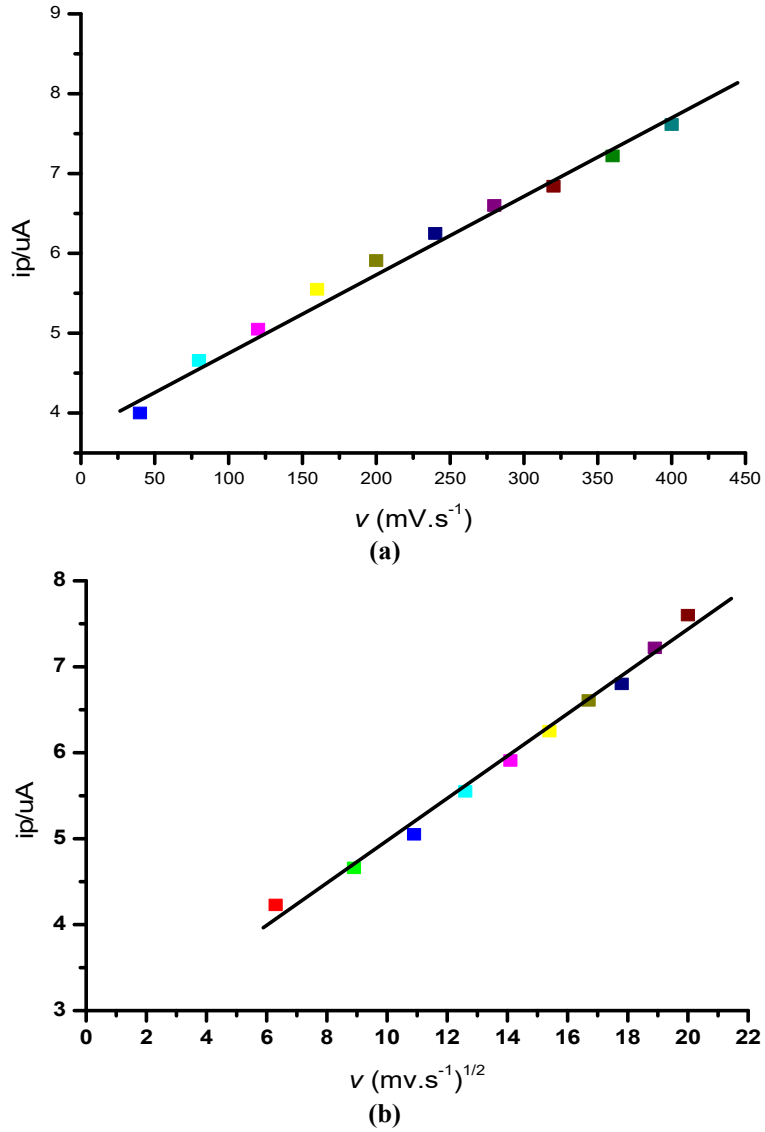

Figure 3: Plot of i_p *vs.* (**a**) SR and **(b)** square root of SR for Aza at an Au electrode.

Oxidation i_p height was observed to grow with SR, as "$(v)^{1/2}$'' and "(v)" of Aza had a good linear relationship. This behaviour was consistent with the notion that Aza species are transported in large quantities on Au electrode by a process that is mostly controlled by diffusion, with some adsorption [18].
According to the slope of i_p vs. $v^{1/2}$, Table 1 shows values of D.

Table 1: Values of electrochemical parameters obtained from ordinary Au electrodes.

k_s^{Ox} m/s^{-1}	$E_{1/2}^{Ox}$ V	D_{Ox} m^2/s^{-1}	α_{Ox}	kc_{Ox} s^{-1}
[a]1.9e - 5	0.540	6.5e-9 [b]6.1e-9	0.39 0.36	4.5

[a] CV data; [b] deconvolutive data

It was found that faster SR (v) increased current and shifted E_p to more positive values. E_p and i_p were highly correlated, although there have been few quantitative studies on this connection. $E_{1/2}$ should be approximately equal to the extrapolation to zero current potential for each straight line [19].
Oxidative transfer coefficients were determined using Eq. (1) [20].

$$E_p - E_{p/2} = 48/\alpha n_a \qquad (1)$$

Additionally, D values were calculated using i_p equation and '$v^{1/2}$' [20] (Table 1). Heterogeneous rate constant k_s values were determined from 'E_p-E_p/2' vs. dimensionless parameter ''ψ'', as established in literature [21].
E_p-E_p/2 values were in the range from 68 to 103 mV, for the chosen SR. They increased with higher SR, as seen in Fig. 4, which led to Aza's redox reaction having a quasi-reversible system for k_s rate.

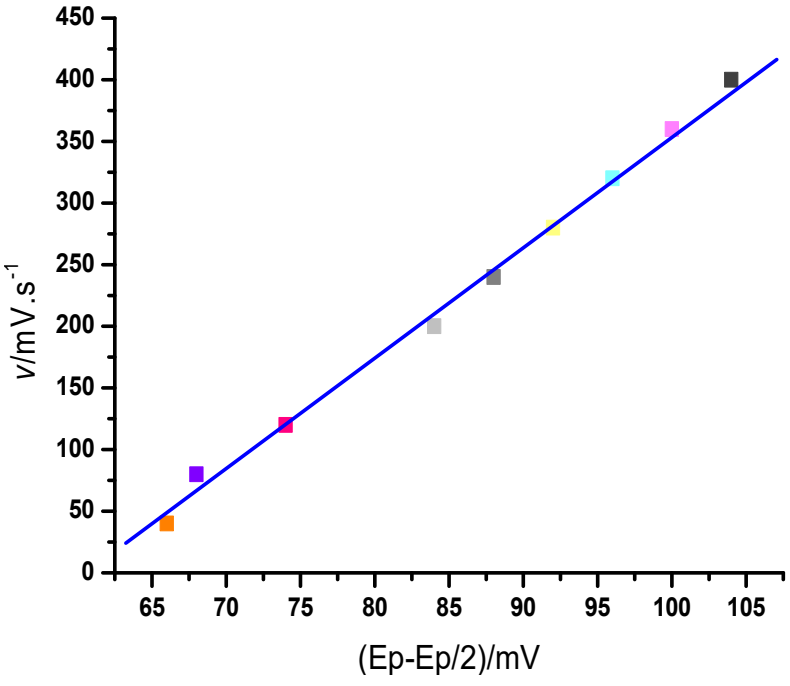

Figure 4: Plot of i_p *vs.* E_p - $E_{p/2}$ of Aza.

Plotting i_{pa} against E_p, as seen in Fig. 5, is one method for assessing potential shift.

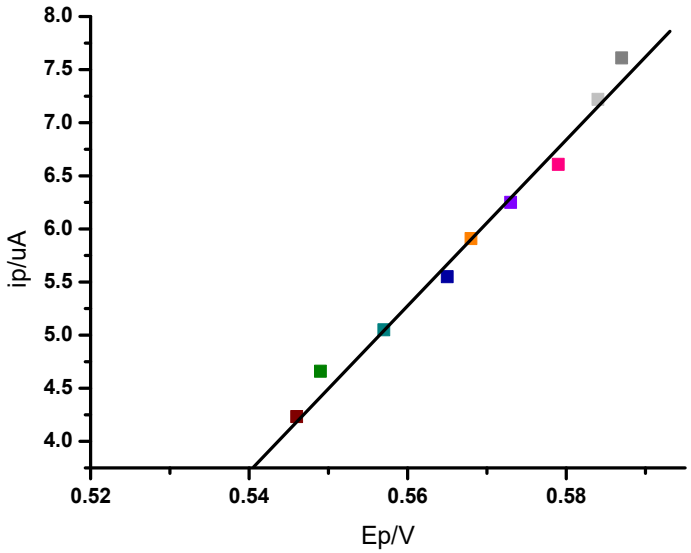

Figure 5: *i*p *vs.* E_p of Aza.

ConvV

CV examination was followed by convolutional mathematical transformation. The method is relatively insensitive to *iR* decrease and yields quantities that are directly connected to the concentration of electroactive species at the electrode surface (as opposed to the flux of a compound, as in original approaches).

In the event of a straightforward electron transfer mechanism for electroactive species *A*, it was discovered that Fick's Second Law might be expressed as [20]:

$$[\partial C_A/\partial t]_x = D_A[\partial^2 C_A/\partial x^2]_x \quad (2)$$

This equation may be solved at the electrode to provide

$$I_1(t) = (C_A^b - C_A(t)).[nFSD_A^{1/2}] \quad (3)$$

where I_1 signifies current semi-integration, which is defined as in [20]:

$$I_1(t) = \pi^{-1/2}\int_0^t [i(u)/(t-u)^{1/2}]\,du \quad (4)$$

Under pure diffusion-controlled situations [i.e., when $C_{(0,t)} = 0$], $I_1(t)$ gives its limiting value, I_{lim}:

$$I_{lim} = nFSC\sqrt{D} \quad (5)$$

Semi-integration changes the shape of the cyclic curve (*i*-*E*) into an S-shaped plot of *I*(*t*)-*E* curve, which results in a steady-state curve and, in some situations, is more adaptable for data processing [20]. To accurately assess $I_1(t)$, Eq. (6) was employed [20]:

$$I(t) = I(k\Delta t) = \frac{1}{\sqrt{\pi}}\sum_{j=1}^{j=k}\frac{\Gamma\left(k-j+\frac{1}{2}\right)}{(k-j)}.\Delta\, t^{1/2} i(j\,\Delta t) \quad (6)$$

The current at equal intervals of time is represented by i(jΔt), while gamma function of x is represented by Γ(x). Aza's I_1 convolution curve at the Au electrode is shown in Fig. 6a, which clearly distinguishes forward and backward sweeps, when driven in the opposite direction [21, 22]. The slow electron transport rate may explain these phenomena. Furthermore, the inclusion of a chemical step in the redox pathway of Aza molecule at the Au electrode surface was confirmed by the fact that the backward scan of I_1 convolution could not return to zero.

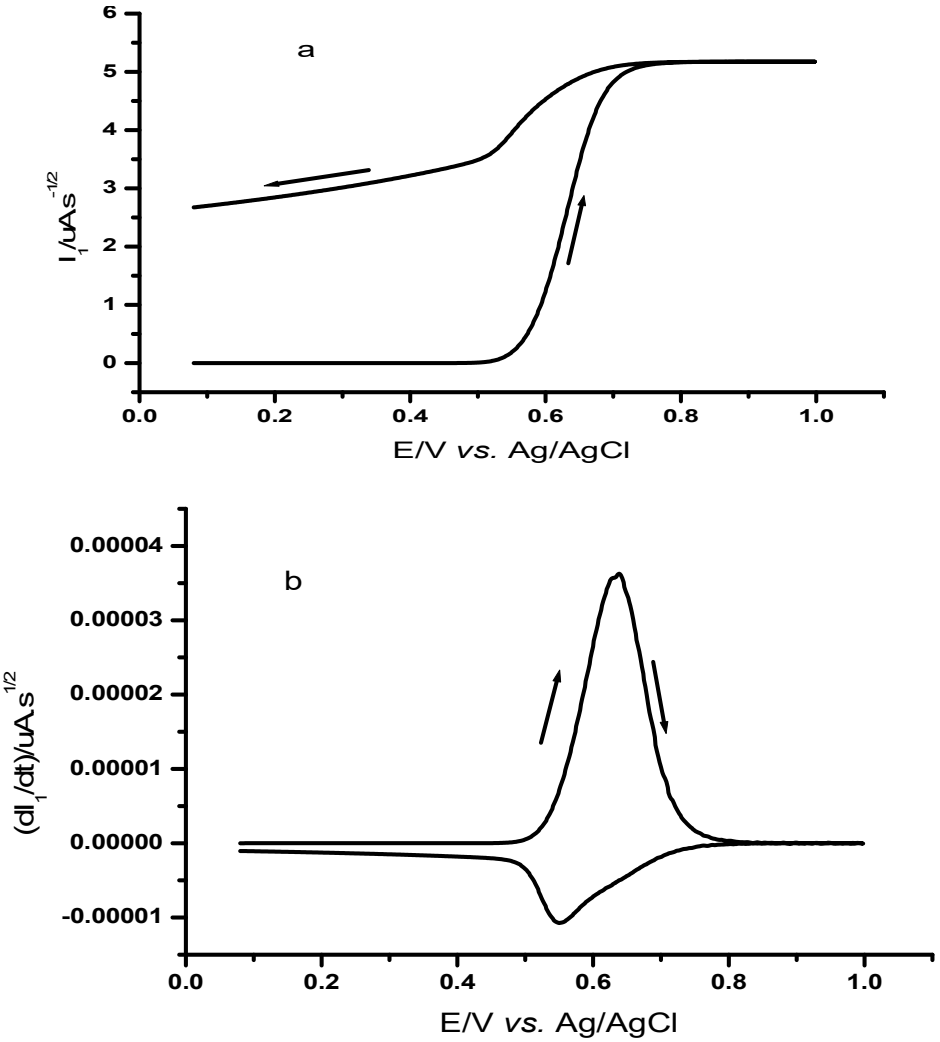

Figure 6: ConvV (a) and DeconvV (b) of Aza at ordinary Au electrode in pH 4.0.

DeconvV was defined as by [23, 24]:

$$(dI_1/dt) = nFAC\sqrt{Da}\zeta / (1+\zeta)^2 \quad (7)$$

The symbols a and ζ are defined as follows:

$$a = nvF/RT \quad (8)$$

$$\zeta = exp\,[nF/RT\,(E - E^0) \quad (9)$$

DeconvV curve at an ordinary Au electrode with v = 320 mV/s^{-1} is displayed in Fig. 6b. The half-width of the deconvoluted peak should be [19]:

$$wp = 2.94\,RT/\alpha n_a F \quad (10)$$

Experimental measurements showed that half-width of the deconvoluted peak at half of its own height (w_p) was 95 mV, indicating that the electron transport of Aza at the Au electrode surface appeared to be moderate. Table 1 contains the values of symmetry factor (α), as determined by Eq. (10). Additionally, the absence of a deconvolutive peak in the reverse direction indicates and validates the conclusion of a quick chemical reaction that followed Aza's electro oxidation. The DeconvV peak height was used for calculating D via Eq. (11) [24] (Table 1).

$$e_p = \frac{\alpha n^2 F^2 v C^{bulk} D^{1/2}}{3.367\,RT} \quad (11)$$

The remaining parameters have their recognized meanings, while the symbol e_p stands for E_p (in amperes). Table 1 lists D values that were established using Eq. (11). The number of electrons engaged in the mechanistic pathway was also determined using Eq. (12).

$$n = \frac{0.086 e_p}{I_{lim}\alpha\, v} \quad (12)$$

For the electrode reaction of Aza, the calculated number of electrons, n, involved in the electrode reaction via Eq. (12), was found to be 2.01. As demonstrated, the aforementioned equation offers an effective and straightforward technique for figuring out how many electrons were spent in the electrode reaction without knowing its surface area. I_1 vs. E and (dI_1/dt) vs. E curves were found to be easier to understand and establish the electrode reaction's nature based on the aforementioned data.

DSM

DSM is a crucial and effective tool for understanding the type of mechanistic pathway of electrode reactions and for theoretic calculation of kinetic parameters [25, 26]. For anodic electrode reactions, the transfer coefficient, $E_{1/2}$, D and heterogeneous rate constants were experimentally calculated and verified by DSM [21, 23, 26]. Electrochemical parameters that showed the least amount of variation between the numerically simulated curves and the experimental plots were compared between experimental and theoretical curves. Wave parameters shown in Table 2 support the proposed mechanism and the reliability of Aza compounds' determined electrochemical properties.

Table 2: simulated and experimental wave parameters.

E_p/V	i_p/uA	$E_p - E_{p/2}$V
[a]0.539	6.900	0.950
[b]0.540	7.100	0.939

[a]Simulated wave parameters; [b]Experimental wave parameters.

Theoretical and recorded experimental CV, as shown in Fig. 7, support the validity of EC mechanistic route of the electrode reaction and the precision of electrochemical parameters experimentally derived.

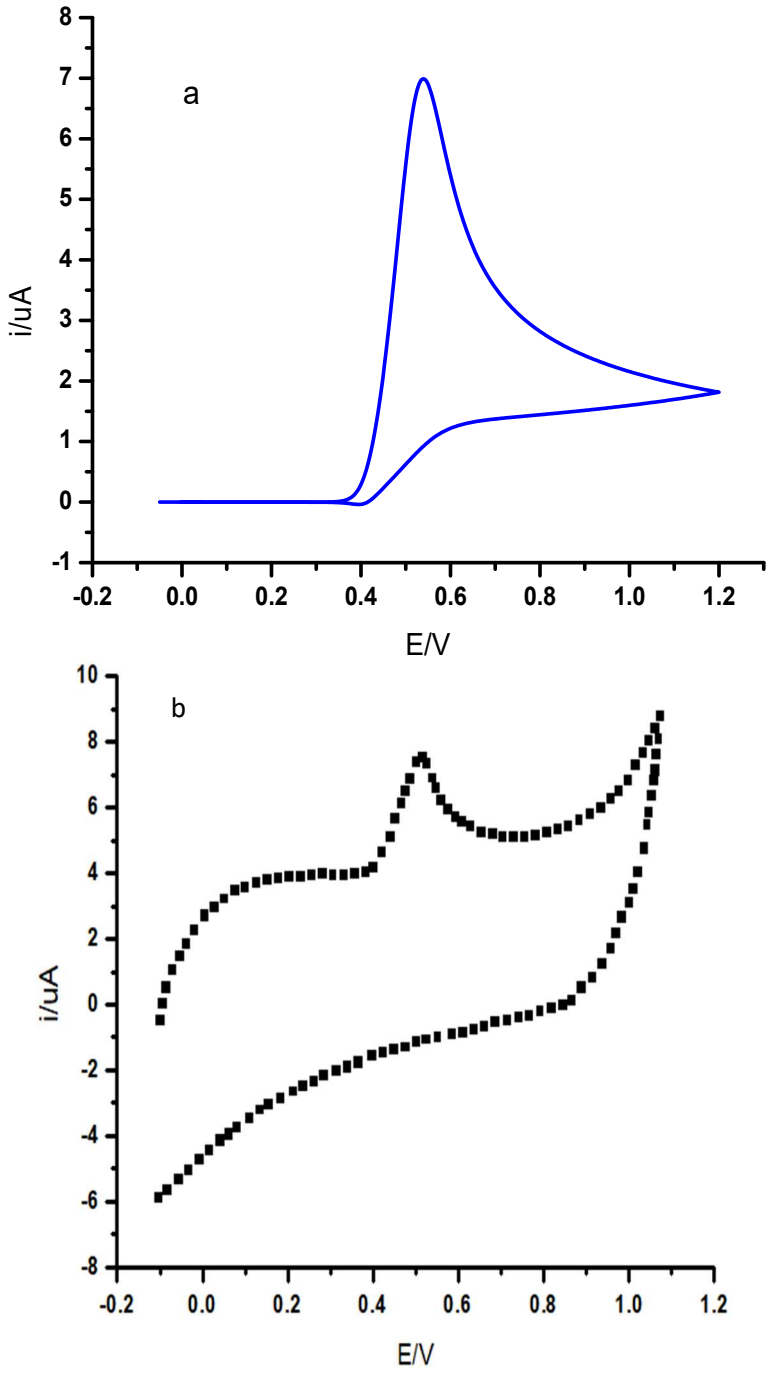

Figure 7: CV of **(a)** simulated and **(b)** experimental Aza at an ordinary Au electrode at a SR of 0.8 V/s^{-1}.

Conclusion

In this article, we studied the 5 x 10^{-6} M Aza electrochemical behaviour at Au electrodes in a pH 4.0 universal BRB solution. This behaviour proves that a chemical process took place after the charge transfer. The accuracy of the electrochemical parameters found experimentally was confirmed, and the mechanistic pathway of the electrode reaction was determined, using the good agreement between theoretical and experimental CV. The observed results suggested that the electrode reaction's mechanistic route should function as an EC mechanism.

Authors' contributions

I. S. El-Hallag: suggested the idea of the article and performed the experimental part. **A. A. Al-Owais**: wrote the article and elucidated the obtained results. **S. H. El-Mossalamy**: performed DSM, revised the article and provided the compound under consideration. **H. M. Hendawy**: revised the article and proof version.

Statements and declarations

The authors declare that they have no known competing financial interests or personal relationships that could have appeared to influence the work reported in this paper.

Funding

Not applicable.

Conflict of interests

The authors declare no conflict of interest.

Abbreviations

Ag: silver
AgCl: silver chloride
Au: gold
Aza: Azapropazone (5-dimethylamino-9-methyl-2-prop-2-enylpyrazolo)
BRB: Britton-Robinson buffer
ConvV: convolution voltammetry
CV: cyclic voltammetry
D: diffusion coefficient
DeconvV: deconvolution voltammetry
DSM: digital simulation method
E1/2: half-wave potential
$\mathbf{E_c}$: electron transfer followed by chemical reaction
EC: electrolysis mechanism
$\mathbf{e_p}$: height of deconvolution voltammetric peak
$\mathbf{E_p - E_p/2}$: half-peak potential width
GCE: glassy carbon electrode
HPLC: high-performance liquid chromatographic method
$\mathbf{I_1}$: convolution current
$\mathbf{i_p}$: peak current
$\mathbf{i_r}$: decrease in effective potential applied to the electrochemical double layer.
KCl: potassium chloride
Ks: heterogeneous electron transfer
Redox: reduction/oxidation reactions
S: surface electrode area
SCE: saturated calomel electrode
SR: scan rate
SWV: square wave voltammetry
TLC: thin-layer chromatography
$\mathbf{w^p}$: half-width of the deconvoluted peak

References

1. Yusuf M, Elfghi FM, Zaidi SA et al. Applications of graphene and its derivatives as an adsorbent for heavy metal and dye removal: a systematic and comprehensive overview. RSC Adv. 2015;5:50392. https://doi.org/10.1039/c5ra07223a
2. Ajmal M, Siddiq M, Aktas N et al. Magnetic Co–Fe bimetallic nanoparticle containing modifiable microgels for the removal of heavy metal ions, organic dyes and herbicides from aqueous media. RSC Adv. 2015;5:43873. https://doi.org/10.1039/C5RA05785J
3. Rosi NL, Giljohann DA, Thaxton CS et al. Oligonucleotide-Modified Gold Nanoparticles for Intracellular Gene Regulation. Science. 2006;312:1027. https://doi.org/10.1126/science.1125559
4. Shchukin DG, Schattka JH, Antonietti M et al. Photocatalytic properties of porous metal oxide networks by nanoparticle infiltration in a polymer gel template. J Phys Chem. 2003;B107:952. https://doi.org/10.1021/jp026929i
5. Mousa SA, Rainsford KD, Timmermans PBM. Pharmacology of azapropazone: potential utility in the treatment of ischemia/reperfusion injury. Cardiovasc Drug Rev. 1992;10:323. https://doi.org/10.1111/j.1527-3466.1992.tb00254.x
6. Olsson S. Recent developments in pharmacovigilance at UMC. In: Vohora D, Singh G, editors. Pharmaceutical medicine and translational clinical research. London: Academic Press; 2018:435-442. eBook ISBN: 978012 802 0982.
7. Testa CJ, Hu C, Shvedova K. Design and commercialization of an end-to-end continuous pharmaceutical production process: a pilot plant case study. Org Process Res Dev. 2020;24:2874. https://doi.org/10.1021/acs. oprd. 0c 00383
8. Sinha S, Vohora D. Drug discovery and development: an overview. In: Vohora D, Singh G, editors. Pharmaceutical medicine and translational clinical research. London: Academic Press. 2018:19-32. ISBN: 9780 12802 1033.
9. Shibata D. Pharmaceutical medicine and translational clinical research. J Evol Med. 9. https://www.ashdin.com/articles/pharmaceuticalmedicine-and-translational-clinical-research.pdf. 2021
10. Musteata FM. Monitoring free drug concentrations: challenges. Bioanalysis. 2011;3:1753. https://doi.org/10.4155/bio.11.187
11. Geissler HE**,** Mutschler E, Faust-Tinnefeldt G. On the determination of azapropazone from plasma by direct quantitative thin-layer chromatography. Arzneim Forsch. 1977;9:1713. PMID: 579143.
12. Geçgel Ü, Özcan G, Gürpınar GC. Removal of Methylene Blue from Aqueous Solution by Activated Carbon Prepared from Pea Shells (*Pisum sativum*). J Chem. 2013;1. https://doi.org/10.1155/2013/614083
13. Malina J, Rađenović A. Kinetic Aspects of Methylene Blue Adsorption on Blast Furnace Sludge. Chem Biochem Eng Quart. 2015;28:491. https://doi.org/10.15255/CABEQ.2014.19366

14. Hendawy H, Amin AA, Dessouki H et al. Electroanalytical determination of Azapropazone at Glassy Electrode Using Differential Pulse and Anodic Square-Wave Voltammetry in Pure Formulation and Pharmaceutical Formula. Sci J Oct 6th Univ. 2017;3(1):28:32. https://doi.org/10.21608/sjou.2017.31575
15. Manjunatha JG, Kumara SBE, Mamatha GP. Electrochemical response of dopamine at phthalic acid and triton X-100 modified carbon paste electrode: a cyclic voltammetry study. Int J Electrochem Sci. 2009;4:1469. https://doi.org/10.1016/S1452-3981(23)15237-0.
16. Charithra MM, Manjunatha JGG, Raril C. Surfactant modified graphite paste electrode as an electrochemical sensor for the enhanced voltammetric detection of estriol with dopamine and uric acid. Adv Pharm Bull. 2020;10:247. https://doi.org/10.34172/apb.2020.029
17. Torriero AAJ, Tonn CE, Sereno L et al. Electrooxidation mechanism of non-steroidal anti-inflammatory drug piroxicam at glassy carbon electrode. J Electroanalyt Chem. 2006;588:218. https://doi.org/10.1016/j.jelechem.2005.12.023
18. EL-Hallag IS, Asiri AM, EL-Mossalamy EH. Data analysis and evaluation of the electrochemical parameters for the ET process via convolutive voltammetry and digital simulation J Chil Chem Soc. 2013;58:921. http://dx.doi.org/10.4067/S0717-97072013000300028
19. El-Hallag IS, Al-Owais AA, El-Mossalamy EH. Electrochemical studies of catechol at ordinary and mesoporous platinum electrodes via convolutive voltammetry and numerical simulation methods. J Solid State Electrochem. 2023;27:3325. https://doi.org/10.1007/s10008-023-05584-w
20. Nicholson RS, Shain I. Experimental verification of an ECE mechanism for the reduction of p-nitrosophenol, using stationary electrode polarography. Analyt Chem. 1965;37:190. https://doi.org/10.1021/ac60221a003
21. Bard AJ, Faulkner LR. Electrochemical Methods: Fundamentals and Applications. John Wiley & Sons. 2001.
22. Leddy J, Bard AJ. Polymer films on electrodes: Part XVIII. Determination of heterogeneous electron transfer kinetics at poly (vinylferrocene) and nafion/Ru $(bpy)^{2+}_3$ polymer-modified. J Electrolanalyt Chem. 1985;189:203-219. https://doi.org/10.1016/ 0368-1874(85)80068-X
23. Garrido JA, Rodriguez RM, Bastido RM et al. Study by cyclic voltammetry of a reversible surface charge transfer reaction when the reactant diffuses to the electrode. J Electroanalyt Chem. 1992;32:19. https://doi.org/10.1016/0022-0728(92)80033-Z
24. Oldham K B, Osteryoung RA. On the determination of kinetic parameters from potential-step and voltage-step measurements. J Electroanalyt Chem. 1966;11:397-405. https://doi. org10.1016/0022-0728(66)80008-6
25. Da-Silva ARL, Dos-Santos AJ, Martinez-Huitle CA. Electrochemical measurements and theoretical studies for understanding the behavior of catechol, resorcinol and hydroquinone on the boron doped diamond surface. RSC Adv. 2018;8:483. https://doi. org/10.1039/C7R-A12257H
26. Abrha T, Pal R, Saini RC. A study on voltametric electro-kinetic mechanism of catechol at ℓ-glutamic acid- carbon paste sensor. J Surface Sci Technol. 2017;33:1. https://doi. org/10.18311/jsst/2017/6187